


 Cite this: *RSC Adv.*, 2019, 9, 11781

CF₃: an overlooked chromophore in VCD spectra. A review of recent applications in structural determination†‡

 Sergio Abbate,^{ID}*^a Giovanna Longhi,^a Giuseppe Mazzeo,^a Claudio Villani,^{ID}^b Silvija Petković^{§c} and Renzo Ruzziconi^{ID}^c

The VCD spectra of several chiral compounds containing the CF₃ group are reviewed and analyzed. The list of compounds contains pharmaceutically relevant molecules as well as simple model molecules, having the value of case studies. In particular we point out the importance of the sign of the VCD band relative to some stretching normal mode of CF₃ in the region 1110–1150 cm^{−1}, as diagnostic of the configuration of stereogenic carbons C* to which the CF₃ group is bound: the correspondence (−) ↔ (*R*) and (+) ↔ (*S*) holds for 100% of 1-aryl-2,2,2-trifluoroethanols. DFT calculations confirm these conclusions, but for the rule established here they serve just as a check. This rule is tested on two new compounds, namely *N*-*tert*-butanesulfinyl-1-(quinoline-4-yl)-2,2,2-trifluoroethylamine, **8**, and 4-[2-(2,2,2-trifluoro-1-hydroxyethyl)pyrrolidin-1-yl]-2-(trifluoromethyl)benzonitrile, **10**, both containing two stereogenic elements, one of them being an asymmetric carbon C* of unknown configuration binding a CF₃ group. Discussion of the general validity of the rule is provided and some further tests are run on compounds in well-established drugs.

 Received 22nd February 2019
Accepted 3rd April 2019

DOI: 10.1039/c9ra01358j

rsc.li/rsc-advances

Introduction

Fluorine is a special atom, sharing some properties with the hydrogen atom (valence, size) but differing significantly in some others, so that, when it is used to replace H, it may change to an important degree some molecular properties, while still preserving or mimicking the minimal steric bulkiness of H and its binding properties. This may justify its large use in medicinal chemistry and in designing new drug molecules.¹ Spectroscopic data help to understand the main chemico-physical properties we are alluding to. Table 1 reports the comparison of observed C–F frequencies ($\nu_{\text{C-F}}$), IR integrated intensities of the CF-stretching mode(s) (*A*),^{2–9} the Atomic Polar Tensor (APT) characteristics of the fluorine

atom, recently studied more thoroughly by updated methods,^{10–12} and bond lengths r_{CF} in simple fluorine-containing molecules.

Data for methane and chloromethane have been added for sake of comparison. For clarity's sake we recall the definition of Atomic Polar Tensor (APT) for atom X³ (particularly referenced to X = F):

$$\begin{aligned} &\frac{\partial \mu_x}{\partial x_X}, \frac{\partial \mu_x}{\partial y_X}, \frac{\partial \mu_x}{\partial z_X} \\ &\frac{\partial \mu_y}{\partial x_X}, \frac{\partial \mu_y}{\partial y_X}, \frac{\partial \mu_y}{\partial z_X} \\ &\frac{\partial \mu_z}{\partial x_X}, \frac{\partial \mu_z}{\partial y_X}, \frac{\partial \mu_z}{\partial z_X} \end{aligned}$$

where μ_x , μ_y , and μ_z are the Cartesian components of the molecular electric dipole moment and x_X , y_X , and z_X are the Cartesian components of the X-atom displacements. Data in Table 1 lend themselves to some considerations. First, while the values of ν_{CH} and ν_{CCl} fall outwardly the spectroscopic ranges crowded with other modes, (column 2) the C–F stretching frequency, ν_{CF} , falls in a quite populated spectroscopic region and consequently couples with several other vibrational modes, so that the influence of fluorine ranges from 1000 to 1500 cm^{−1}. Second, the IR-absorption intensity associated with CF-stretching is larger than those of either C–H or C–Cl stretching in methane or other methyl halides, like chloroform (column 3), the same happens for C–Br and C–I stretching in

^aDMMT (Dipartimento di Medicina Molecolare e Traslazionale), Università di Brescia, Viale Europa 11, 25123 Brescia, Italy. E-mail: sergio.abbate@unibs.it

^bDipartimento di Chimica e Tecnologie del Farmaco, Università di Roma “La Sapienza”, Piazzale Aldo Moro 5, 00185 Roma, Italy

^cDipartimento di Chimica, Biologia e Biotecnologie, Università di Perugia, Via Elce di Sotto 8, 06123 Perugia, Italy

† Work presented in part at the International VOA-6 Conference held in Brescia, Italy, in September 9–13, 2018.

‡ Electronic supplementary information (ESI) available: Experimental VCD and IR spectra of enantiomers and diastereomers (when available) of compounds **8** and **9** and diastereomers of (X,Y)-2-acetyl-N-(*tert*-butanesulfinyl)-3-oxo-1-(trifluoromethyl)butylamine.⁵⁴ See DOI: 10.1039/c9ra01358j

§ At the time the research was carried out, SP was an Erasmus student from University of Zagreb, Croatia, visiting the lab in Perugia, Italy, headed by RR.



Table 1 Important parameters from IR spectroscopy of molecules containing CF bonds. Analogous characteristics for reference molecules are reported for comparison^a

Compound (ref.)	ν_{CX} (cm ⁻¹)	A (km mol ⁻¹)	p_{Av} (e)	β (e)	χ (e)	r_{CX} (Å)
CH ₄ (⁴)	3019	69.7	-0.004	0.670	0.019	1.090
CH ₃ Cl (⁵)	738	23.4	-0.268	0.175	0.298	1.780
CH ₃ F (³ and ⁶)	1063	96.3	-0.479	0.605	0.557	1.382
CH ₂ F ₂ (³ and ⁷)	1090, 1111	311.9	-0.488	0.640	0.574	1.351
CHF ₃ (³ and ⁸)	1150 ($\nu_2 + \nu_5$)	626.8	-0.505	0.670	0.595	1.332
CF ₄ (³ and ⁹)	1280	1080.0	-0.512	0.410	0.547	1.329

^a ν_{CX} (cm⁻¹) = observed IR frequency values; A (km mol⁻¹) = observed IR intensity values; p_{Av} (e) = average value of the Atomic Polar Tensor (APT) for F atom (or for H in CH₄, or for Cl in CH₃Cl). First (Linear) invariant of APT; β (e) = anisotropy (second (quadratic) invariant) of APT for F atom (or for H in CH₄, or for Cl in CH₃Cl). χ (e) = third (cubic) invariant of APT for F atom (or for H in CH₄, or for Cl in CH₃Cl). r_{CX} (Å) = equilibrium bond length for CX bond (X = F or H in CH₄, or for Cl in CH₃Cl). [e = charge of the electron.]

analogous circumstances. Moreover, by adding one CF at a time, from CH₃F to CH₂F₂, to CHF₃ to CF₄ the intensity does not increase by the same amount, but an increasing gradient can be noticed, namely by 216 km mol⁻¹ from CH₃F to CH₂F₂, by 315 km mol⁻¹ (+99 km mol⁻¹ for gradient) from CH₂F₂ to CHF₃, and by 453 km mol⁻¹ (+138 km mol⁻¹ for gradient) from CHF₃ to CF₄, that turns out into an increasing values for APT invariants. Third, let us indeed consider in column 4 of Table 1 the mean dipole moment derivative with respect to F-displacements, $p_{\text{Av}}(\text{F})$:

$$p_{\text{Av}}(\text{F}) = \frac{\partial \mu_x}{\partial x_{\text{F}}} + \frac{\partial \mu_y}{\partial y_{\text{F}}} + \frac{\partial \mu_z}{\partial z_{\text{F}}},$$

the anisotropy (column 5, Table 1):

$$\beta^2(\text{F}) = (1/2) \left[\left(\frac{\partial \mu_x}{\partial x_{\text{F}}} - \frac{\partial \mu_y}{\partial y_{\text{F}}} \right)^2 + \left(\frac{\partial \mu_x}{\partial x_{\text{F}}} - \frac{\partial \mu_z}{\partial z_{\text{F}}} \right)^2 + \left(\frac{\partial \mu_z}{\partial z_{\text{F}}} - \frac{\partial \mu_y}{\partial y_{\text{F}}} \right)^2 \right. \\ \left. + 3 \left(\left(\frac{\partial \mu_x}{\partial y_{\text{F}}} \right)^2 + \left(\frac{\partial \mu_y}{\partial x_{\text{F}}} \right)^2 + \left(\frac{\partial \mu_x}{\partial z_{\text{F}}} \right)^2 + \left(\frac{\partial \mu_z}{\partial x_{\text{F}}} \right)^2 + \left(\frac{\partial \mu_y}{\partial z_{\text{F}}} \right)^2 + \left(\frac{\partial \mu_z}{\partial y_{\text{F}}} \right)^2 \right) \right]$$

and the effective charge $\chi(\text{F})$ (column 6), whose square is defined as 1/3 the trace of the APT square of fluorine atom; it should be noted that $p_{\text{Av}}(\text{F})$, $\beta(\text{F})$ and $\chi(\text{F})$ are invariant with respect to Cartesian axes choice. Not only the charge of the fluorine atom is *ca.* -0.5 e and it increases in going from CH₃F to CF₄ with negative sign (as experimentally determined¹³⁻¹⁵), but fluorine exhibits also a large anisotropy, that means a large

polarizability and a propensity to form hydrogen bonding.¹² All these properties have been verified through DFT. In Table 2 we compare our own DFT calculated fundamental C-F stretching frequencies and the corresponding IR absorption intensities with the corresponding observed experimental data in the gas phase. Interestingly, irrespective of the fact that anharmonicity (neglected here) generally has the effect of decreasing their values, calculated frequencies are smaller than the observed ones, while the opposite happens for the intensities. In any case frequency values differ from the observed ones by 5% at most, while IR intensities by *ca.* 10%.

Fourth point, but not the least, the length of the CF bond is progressively shorter as the number of C-F bonds (7th column in Table 1). This means a stronger C-F bond, which parallels the increasing value of ν_{CF} and increased effective charge value as well. From all the above properties, especially the large anisotropy, the presence of fluorine atoms is expected to affect the VCD spectra of organic molecules to a greater extent.

VCD is a technique,¹⁶⁻¹⁸ which, in conjunction with density functional theory (DFT) calculations, has emerged in the last 30 years as a powerful tool to investigate chiral molecules.¹⁹⁻²² Usually, it is applied together with other chiroptical techniques, like electronic circular dichroism (ECD) or optical rotatory dispersion (ORD).^{23,24}

In this review we focus our attention onto a particular class of molecules bearing the CF₃ group bound to a stereogenic carbon. The introduction of a CF₃, into a structure of potentially bio-active compound, is an established paradigm in the modern medicinal chemistry and drug-design.²⁵⁻²⁷ Its use in medicinal chemistry dates almost a century, although the research became

Table 2 Comparison of calculated and experimental CF-stretching frequencies and of infrared intensities for fundamental transitions in CH₃F, CH₂F₂, CHF₃ and CF₄^a

Compound	ν_{CF} (cm ⁻¹) observed	ν_{CF} (cm ⁻¹) calculated	A (km mol ⁻¹) observed	A (km mol ⁻¹) calculated
CH ₃ F (³ and ⁶)	1063	1043	96.3	111
CH ₂ F ₂ (³ and ⁷)	1090, 1111	1067, 1103	89.5 + 230.4, $\Sigma = 319.9$	110 + 265, $\Sigma = 375$
CHF ₃ (³ and ⁸)	1150	1129, 1130	$\Sigma = 626.8$	110 + 642, $\Sigma = 752$
CF ₄ (³ and ⁹)	1280	1247	1080	1362

^a Calculations run by use of Gaussian09;²² computational level B3LYP/TZVP (see also Table 1).



evermore intensive since the half of the past century. The trifluoromethyl group is often used as an isostere of iodine or an isopropyl group,²⁸ bringing, however, the beneficial properties of fluorine. This is why it can be found in several agrochemicals, and patent drugs, encompassing Efavirenz, a HIV reverse transcriptase inhibitor; Befloxatone, a reversible inhibitor of monoamine oxidase A; Bitopertin, a glycine reuptake inhibitor; Ligandrol, for treatment of muscle wasting and osteoporosis; Mapracorat, an anti-inflammatory drug. In those drugs a CF₃ group was added bound to a stereogenic carbon, and some of them were studied by VCD in a recent comprehensive paper.²⁹

We feel that VCD is a privileged technique particularly suitable for the recognition of molecules containing CF₃, since there is no specific electronic chromophore associated with this group to make the ECD technique competitive. Finally, we also surmise that some information may be gathered from VCD spectra about the interaction of the CF₃ group with the molecular environment and this may be tied up with pharmacological properties of some drugs.

We shall consider the VCD spectra of some molecules containing CF₃ groups, studied so far by this technique: from Table 1 we learn that the absolute value of the fluorine atomic charge in the CF₃ group, as well as its anisotropy, are the highest among the fluorinated groups. The molecules whose VCD data will be discussed here, are depicted in Scheme 1, and are classified as follows: group **A**, previously studied pharmacologically important molecules (1 and 2); group **B**, previously studied molecules (3–7), exhibiting some relevant chiroptical and hydrogen bond properties established through VCD, IR spectroscopies and DFT calculations; group **C**, novel compounds (8

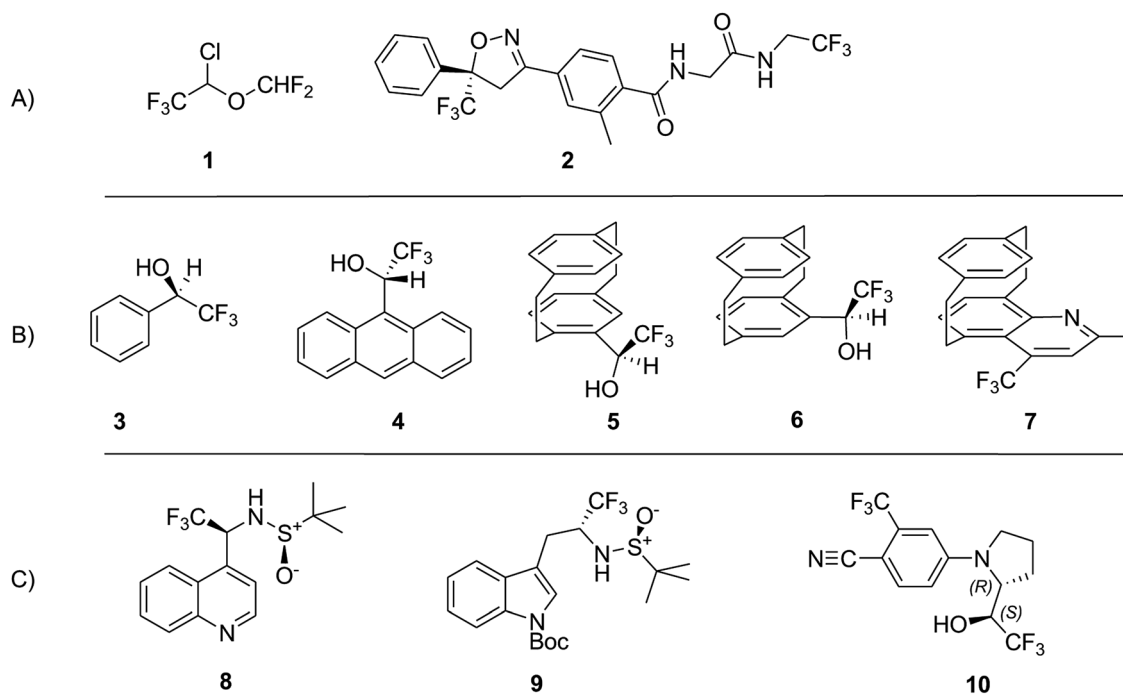
and 10) studied by VCD here for the first time, plus a congener of 8, namely 9, which had been previously studied.³⁰ The latter three compounds exhibit two stereogenic centers: in the sulfonamides 8 and 9 one stereocenter is the sulfur atom of a sulfonamide group of known AC and the additional stereogenic carbon binds a CF₃ group.

Experimental

All data referring to the molecules 1–7 in Scheme 1 is from the literature. They are presented here and re-discussed in order to find a “*fil rouge*” binding several different instances.

Data for stereoisomeric *N-tert*-butanesulfinyl-1-(quinoline-4-yl)-2,2,2-trifluoroethylamines (8) (Scheme 1) are fully commented in the present work for the first time, since the synthesis and properties thereof had never been investigated, while its “sister” molecule 9 was already studied in a previous work.³⁰ Diastereomeric (*X,R_S*)- and (*Y,R_S*)-*N-tert*-butanesulfinyl-1-(quinoline-4-yl)-2,2,2-trifluoroethylamine (8) were obtained from the addition of 4-lithioquinoline to *N-tert*-butanesulfinyltrifluoroacetaldehyde according to the following Scheme 2.

tert-Butyllithium (1.63 M in hexanes, 3.00 mL, 4.89 mmol) was added drop-wise in 5 min to a solution of 4-bromoquinoline (1.00 g, 4.81 mmol) in diethyl ether (22 mL) at –100 °C. After 90 min stirring at the same temperature, a solution of (*R*)-*N-tert*-butanesulfinyltrifluoroacetaldehyde (1.00 g, 4.97 mmol) in diethyl ether (3 mL) was added, and the reaction mixture was stirred further for 90 min. The cold bath was removed and the temperature was allowed to rise to 25 °C before brine (25 mL) was added. The organic phase was separated and extracted with



Scheme 1 Examples of CF₃-containing molecules, whose VCD was already studied or is under study. Line (A) pharmacologically relevant molecules (1, 2); line (B) prototypical CF₃-containing molecules (3–7) for which extensive VCD studies were conducted; line (C) sulfonamides (8 and 9) containing a CF₃ groups at a chiral carbon and a stereogenic sulfur of known configuration. 4-((*R*)-2-((*S*)-2,2,2-Trifluoro-1-hydroxyethyl)pyrrolidin-1-yl)-2-(trifluoromethyl)benzonitrile (10), the configuration of which is determined here.



diethyl ether (3 × 25 mL), the collected organic phases were dried over Na₂SO₄ and the solvent was evaporated at reduced pressure. The remaining consisted mainly of a mixture of two diastereomeric products in 8 : 2 molar ratio as determined by ¹⁹F NMR analysis. Chromatography on silica gel (eluent mixture, diethyl ether/ethyl acetate = 7 : 3) allowed to separate a white solid (1.03 mg; 65%), mp > 250 °C as the first eluted product exhibiting the following analytic and spectroscopic characteristics.

(*X,R_S*)-*N*-*tert*-Butanesulfinyl-1-(quinoline-4-yl)-2,2,2-trifluoroethylamine [(*X,R_S*)-**8**], white rhombic crystals; mp > 250 °C, [α]_D²⁴ = +85 (*c* = 0.5, CH₃OH). ¹H NMR δ 9.03 (d, *J* = 4.6 Hz, 1H), 8.25 (d, *J* = 8.5 Hz, 1H), 8.14 (d, *J* = 8.6 Hz, 1H), 7.83 (t, *J* = 8.1 Hz, 1H), 7.70 (t, *J* = 8.2 Hz, 1H), 7.65 (d, *J* = 4.6 Hz, 1H), 5.80 (m, 1H), 4.13 (bd, *J* = 4.1 Hz, 1H), 1.26 (s, 9H); ¹³C NMR δ 149.6, 148.5, 137.9, 130.5, 130.0, 127.8, 126.6, 124.3 (q, *J* = 280 Hz), 122.6, 121.3, 56.9, 55.4 (broad), 22.3 (3C); ¹⁹F NMR δ -72.44 (bd, *J* = 7.1 Hz, 3 F). Elemental analysis, calcd for C₁₅H₁₇F₃N₂OS (330.37): C, 54.53; H, 5.19; N, 8.48. Found: C, 54.71; H, 5.25; N, 8.37. The second eluted product was obtained as yellow thick oil (0.26 g; 16%). (*Y,R_S*)-*N*-*tert*-butanesulfinyl-1-(quinoline-4-yl)-2,2,2-trifluoroethylamine [(*Y,R_S*)-**8**, 16%]. [α]_D²⁴ = -201 (*c* = 0.5, CH₃OH). ¹H NMR δ 9.00 (d, *J* = 4.5 Hz, 1H), 8.25 (d, *J* = 8.1 Hz, 1H), 8.19 (d, *J* = 8.5 Hz, 1H), 7.84 (t, *J* = 7.9 Hz, 1H), 7.74 (t, *J* = 7.0 Hz, 1H), 7.61 (d, *J* = 4.5 Hz, 1H), 5.75 (quint, *J* = 6.7 Hz, 1H), 3.99 (d, *J* = 6.4 Hz, 1H), 1.28 (s, 9H); ¹³C NMR δ 149.3, 130.4, 130.2, 129.7, 128.2, 126.4, 125.7, 124.4 (q, *J* = 280 Hz), 122.5, 119.6, 57.4, 55.5 (q, *J* = 31 Hz), 22.3 (3C); ¹⁹F NMR δ -72.50 (d, *J* = 7.2 Hz, 3 F). Elemental analysis, calcd for C₁₅H₁₇F₃N₂OS (330.37): C, 54.53; H, 5.19; N, 8.48. Found: C, 54.64; H, 5.27; N, 8.54.

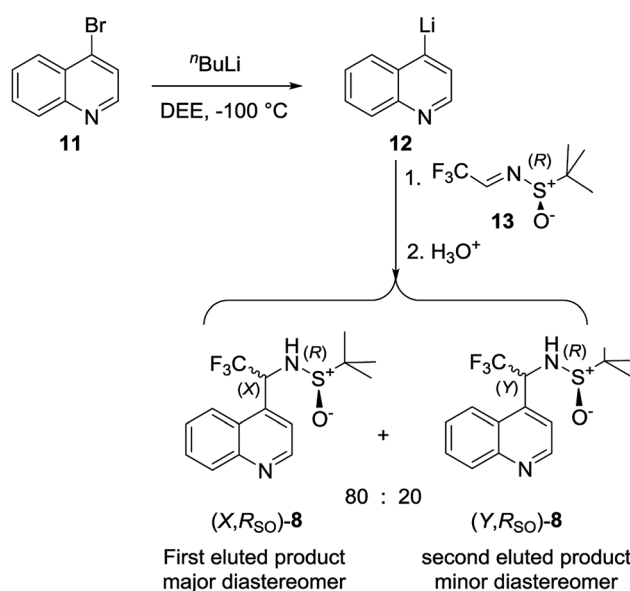
In the same way, diastereomeric (*X,S_S*)- and (*Y,S_S*)-*N*-*tert*-butanesulfinyl-1-(quinoline-4-yl)-2,2,2-trifluoroethylamine were obtained, in practically the same dr ratio and with satisfactory yields, starting from 4-bromoquinoline and (*S*)-*N*-*tert*-butanesulfinyltrifluoroacetalimine. Their spectroscopic characteristics were identical to those reported above for (*X,R_S*)-**8** and (*Y,R_S*)-**8**, respectively. Elemental analysis, calcd for C₁₅H₁₇F₃N₂OS (330.37): C, 54.53; H, 5.19; N, 8.48. Found, (*X,S_S*)-**8**: C, 54.53; H, 5.19; N, 8.48; (*Y,S_S*)-**8**: C, 54.68; H, 5.27; N, 8.36.

IR and VCD spectra were performed in CDCl₃ solutions (*ca.* 0.08 M) in 200 μ m-path length BaF₂ IR cells and registered with a Jasco FVS-6000 apparatus, as the results of 5000 accumulated and averaged scans. Subtraction of the solvent was carried out both in the IR and in the VCD spectra, 4 cm⁻¹ resolution was kept. DFT calculations were carried out by the use of Gaussian09, G09 for short;²² the MM analysis allowed a first screening of several conformers, then the use of the G09 module at the PBE0/TZVP/PCM(CH₃Cl) level allowed to select 9 conformers for (*R*)-configuration arbitrarily assigned to the C*(CF₃) stereogenic carbon and 6 conformers for the (*S*)-configuration. Rotational strengths were calculated through G09, based on Stephens' algorithm, PCM approximation being adopted. IR and VCD spectra were generated with a program resident in the Jasco VCD software package and compared with the corresponding experimental data, assuming a bandwidth of 10 cm⁻¹, and with constant scaling factor of 0.98. ECD and UV

measurements were performed in acetonitrile solutions (*ca.* 0.005 M) in 0.1 mm quartz cuvette. ECD-UV calculated spectra were treated with SpecDis.³¹

Compound **10**, (4-[2-(2,2,2-trifluoro-1-hydroxyethyl)pyrrolidin-1-yl]-2-(trifluoromethyl)benzonitrile) was bought from Carbosynth, Gijanshu, China, and its integrity and structure was checked by NMR. We verified the compound to be optically inactive, by measuring all chiroptical properties available to us (OR, ECD and VCD). We thus attempted the separation of its four expected stereoisomers by HPLC on achiral and on chiral stationary phases. Chromatographic analysis on either bare silica or reversed C18 stationary phases always afforded a single, homogeneous peak. Chromatographic analysis on a chiral stationary phase (Chiralpak IA, 250 × 4.6 mm column, eluent hexane/CHCl₃ 1/1, flow rate 1.0 mL min⁻¹) gave two equally intense peaks, oppositely signed when monitored by circular dichroism, with retention times of 17.9 and 20.3 minutes for the first and second eluted, respectively. The analytical separation was scaled up on a semi-preparative column (Chiralpak IA, 250 × 10.0 mm column) giving 12.4 mg of the 1st eluted species with e.e. = 99.3%, and 13.8 mg of the second eluted one with e.e. = 95.5%. OR values, in chloroform solution, were measured at 589, 405 and 365 nm. First eluted (*c* 0.14): +68.4 (589 nm), +296.4 (405 nm) and +584.6 (365 nm). Second eluted (*c* 0.138): -64.3 (589 nm), -250.3 (405 nm) and -510.8 (365 nm). Taken together, chromatographic and polarimetric data indicate that compound **10** is a single diastereoisomer with racemic composition, either (*R,S*)/(*S,R*) or (*R,R*)/(*S,S*).

IR and VCD spectra of **10** were measured with the same apparatus and cell as for **8**. The same computational protocol described above was followed, assuming either (*R,R*) or (*R,S*) as the configurational options, the second stereogenic center referring to the CF₃-bearing carbon. For both options we considered all conformers, details are reported in the next



Scheme 2 Synthesis of (*X,R_S*)- and (*Y,R_S*)-*N*-*tert*-butanesulfinyl-1-(quinoline-4-yl)-2,2,2-trifluoroethylamine.



section. In addition, a similarity analysis was also carried out. For the carbinol **10** calculations were effected using the functional M06-2X, as suggested recently by Kreienborg and Merten.³² Finally, in order to further strengthen our assignment, ECD spectra were also recorded with a Jasco 815SE instrument using *ca.* 0.0045 M acetonitrile solutions in 0.1 mm quartz cuvette. The conformer distribution was inferred from the B3LYP/TZVP/PCM (acetonitrile) and calculated ECD spectra from the CAM-B3LYP/TZVP/PCM (acetonitrile).

Discussion

The polyhalogenated ether **1** (Isoflurane®) is a widely used anesthetic³³ and the diamide **2** (Fluralaner®) is used in veterinary medicine.³⁴ Of course, they are not the only CF₃ containing drugs submitted to VCD investigations,^{35,36} but, as far as we

know, they are the first and the latest, respectively, to be investigated by this technique. In particular we would like to point out the systematic and complete contribution of Polavarapu and collaborators, who, at the offset of the VCD-DFT approach, established not only the absolute configuration (AC) of isoflurane, but also that of desflurane and 1,2,2,2-tetrafluoroethyl methyl ether by discussing also their relationship with 1-methoxytetrafluoropropionic acid, another anesthetic of the same family.^{37–39} The VCD and IR spectra of isoflurane and fluralaner are reported on the left and on the right, respectively, of Fig. 1.

Though we do not intend effecting here a detailed analysis of the spectra of the products in Fig. 1, we note that they exhibit some important peculiarities, which are also present in the model compounds 3–7 with which the VCD technique has been tested for years. The first consideration involves the most

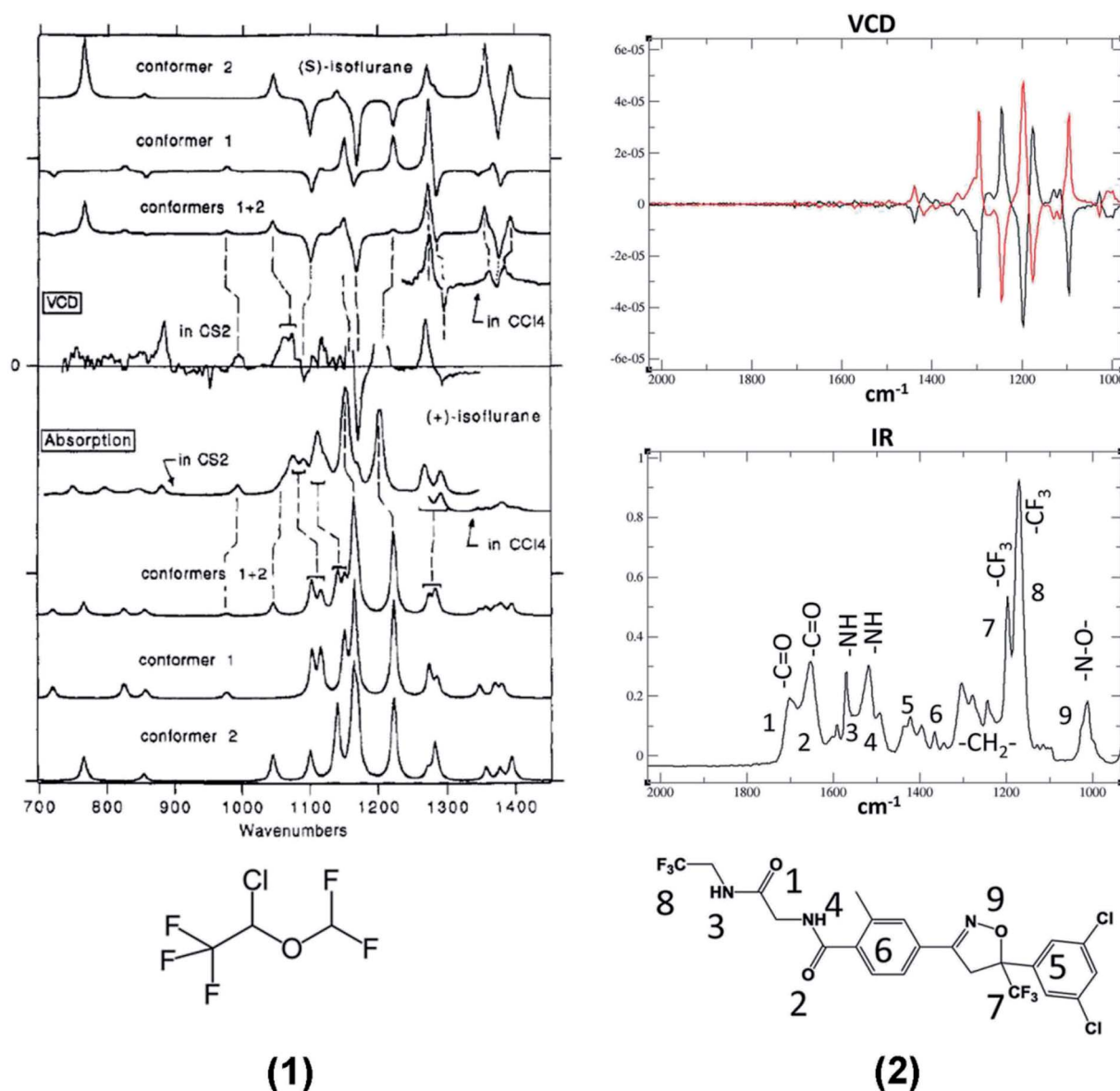


Fig. 1 Left: VCD (top) and IR experimental and calculated spectra of Isoflurane, **1**.³³ Right: VCD (top) and IR experimental spectra of (±)-Fluralaner, **2**.³⁴ (Please notice that the wavenumber scales are in reversed order in the two spectra.)

intense IR doublet between 1100 and 1200 cm^{-1} in the spectra of molecules **1** and **2**, both exhibiting a negative-positive couplet in their VCD spectra due to the antisymmetric and symmetric C–F stretching modes of the CF_3 group (see Table 1). The signed character of VCD in this region gives to this couplet a relevant diagnostic value for the assignment of the absolute configuration at the stereogenic carbon bearing a CF_3 group. Some similarities appear also in the IR and VCD spectra in the range 1200 and 1400 cm^{-1} , where methine (isoflurane) and methylene (fluralaner) C–H bending modes are present.

The examination of the model compound **3–7** is motivated by the search for common features in the IR and VCD spectra of molecules containing CF_3 groups. In Fig. 2 we juxtapose the IR

and VCD spectra of both the enantiomers of 2,2,2-trifluoro-1-phenylethanol **3**, (top) and of 1-phenylethanol (bottom).

These spectra have been recorded and analyzed by several authors. We report our own data for 2,2,2-trifluoro-1-phenylethanol in the mid-IR region,⁴⁰ while data for 1-phenylethanol is from Polavarapu's work.³⁸ Spectral data of 2,2,2-trifluoro-1-phenylethanol in the CH-stretching region are taken from the classical work of Nafie, Keiderling and Stephens,⁴¹ and those for 1-phenylethanol is from the nice work of Pultz.⁴² Referring to the CH-stretching region, we notice that the IR and VCD data of both 2,2,2-trifluoro-1-phenylethanol, **3**, and 1-phenylethanol are fairly similar, that means fluorine has little influence, if any, on the C–H stretching region; the VCD

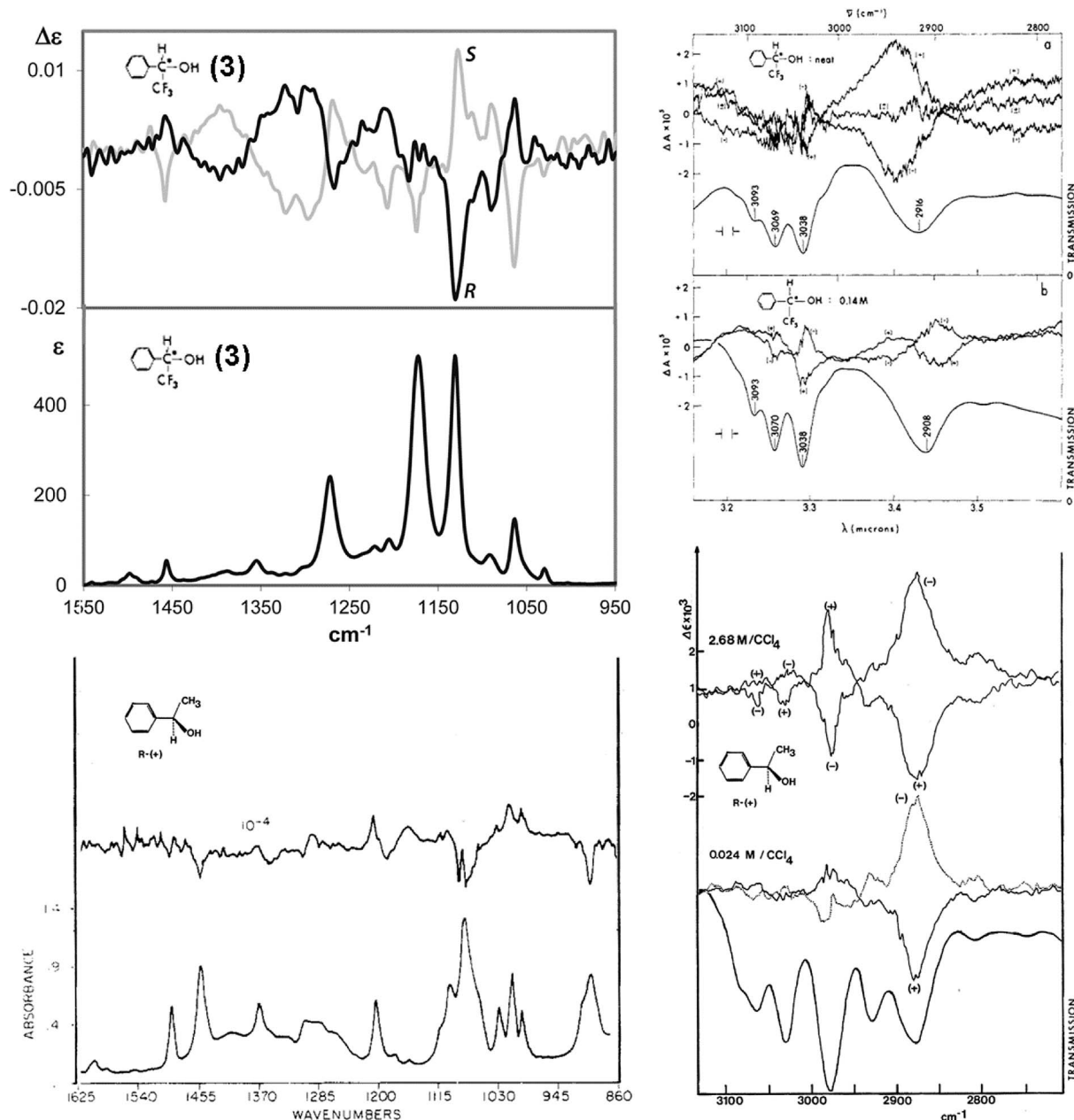


Fig. 2 IR and VCD experimental spectra of the enantiomers of both 2,2,2-trifluoro-1-phenylethanol (**3**) (top) and 1-phenylethanol (bottom). Left, mid-IR region; right: CH-stretching region. (Data from ref. 38, 40–42.)



spectrum is dominated by the C*–H stretching vibration, as proposed by Nafie and collaborators^{43,44} and verified by selectively deuterated analogues,⁴⁵ though there is a remarkable dependence from the concentration. Unlike the CH-stretching region, the mid-IR region is influenced considerably by the presence of the CF₃ group: overall, in that region the intensity is increased, as expected on the basis of the data of Tables 1 and 2. We also notice that the CF₃-symmetric and antisymmetric stretching normal modes contributing to the IR and VCD bands at *ca.* 1130 and 1180 cm^{−1} are degenerate for CHF₃ and are observed at \sim 1150 cm^{−1} (Tables 1 and 2); the degeneracy is relieved by the interaction with adjacent groups, in particular with the polar OH-group competing with the electron-rich phenyl moiety. The IR intensity of the two components is much higher than that of all the other bands and the spectrum of 2,2,2-trifluoro-1-phenylethanol contains VCD bands which are stronger than those of 1-phenylethanol. In general, the VCD spectrum of 2,2,2-trifluoro-1-phenylethanol is quite different from that of 1-phenylethanol (see Fig. 2). No doubt, the presence of the CF₃ group contributes substantially to increase the intensity of the VCD spectrum as a whole and it is easy to give a clear diagnostic value for AC assignment to the clearly defined and intense feature (at \sim 1130 cm^{−1}) nearby the observed CF₃-symmetric stretching frequency in CHF₃ (\sim 1150 cm^{−1}). Namely, it has a negative sign for the (−)-(R) enantiomer and a positive sign for the (+)-(S) enantiomer. On the contrary, the feature at *ca.* 1180 cm^{−1} is weaker, and the sign is opposite to that of the other CF₃-stretching component (Fig. 1). The new peculiar aspect of these two VCD bands ascribed to CF₃-stretching normal modes, which is different from the perfectly bisignated aspect of Fig. 1, is due to the surrounding groups: the CF₃ group attracts intramolecularly^{6,40,46} the OH group and competes effectively with the adjacent phenyl group; the propensity of CF₃ to form H-bonding has a nice counterpart in the anisotropic character of the F-atom APT obtained through IR intensity analysis and evidenced in Table 1. In addition, the VCD intensification noticeable also in the rest of the spectrum at higher wavenumbers, in particular the broad and intense couplet between 1260 and 1430 cm^{−1}, takes on some diagnostic value for the configuration assignment.

Similar phenomena are observed for other carbinols having the CF₃ group bound to the α carbon. Fig. 3 shows the VCD and IR spectra of three chiral aryl (trifluoromethyl)carbinols, with the aryl group being phenyl (3), anthryl (4) and [2.2]paracyclophan-4-yl (5 and 6).⁴⁰ In the first two cases the band at *ca.* 1130 cm^{−1} is intense in IR and VCD and exhibits a negative VCD sign for the (−)-(R)-enantiomer and the positive sign for the (+)-(S)-enantiomer. In the case of 2,2,2-trifluoro-1-(anthr-9-yl)ethanol the IR band is split and the VCD band is centered at \sim 1100 cm^{−1} and its value appears indisputable for AC assignment. The VCD component at higher wavenumber (\sim 1200 cm^{−1}), attributed to the other CF₃-stretching component, is much weaker, though still intense in the IR, and exhibits the reversed sign with respect to the symmetric component; its value is less important for AC assignment compared with the lower frequency CF-stretching band. Even the very broad VCD band centered at \sim 1300 cm^{−1} shows the

same sign in the two molecules and thus is related to AC only, namely, it is positive for the (−)-(R)- and negative for the (+)-(S)-enantiomer.

The case of 2,2,2-trifluoro-1-([2.2]paracyclophan-4-yl)ethanol 5 is slightly more complex, since the [2.2]paracyclophan-4-yl group adds a new stereogenic element, namely the planar chirality of paracyclophane moiety. We demonstrated how much the planar chiral paracyclophane moiety can help the AC assignment at the stereogenic carbon bound to it.⁴⁰ In this case, VCD proved to be more effective than NMR in the AC assignment, which was further confirmed by X-ray. The VCD band at \sim 1100 cm^{−1} containing the low-energy CF₃-stretching normal mode is negative for (*R_p*,*R*) configuration, though with small intensity (bottom left in Fig. 3) and corresponds to (−) optical rotation. In the case of carbinol (*S_p*)-5, the VCD band at *ca.* 1100 cm^{−1} containing a low-energy CF₃-stretching normal mode is more representative; it is negative for (*S_p*,*R*) AC (bottom right part of Fig. 3), it is quite intense and corresponds to (+) optical rotation. Here the 1100 cm^{−1} VCD band is Occam's resolving criterion for AC assignment to an ArC*H(CF₃)OH system; in the previous case the criterion is still applicable, though the VCD band is weak. Ultimately, this is due to different interactions of the CF₃ group with the neighbouring groups because of the different planar chirality.⁴⁰ Other intense VCD bands may be useful for AC assignment, especially those at \sim 1250 cm^{−1}, due to the C–F intensification phenomenon discussed above; it might be observed that the C–F stretching band frequency (\sim 1250 cm^{−1}) is close to the value observed for the C–F stretching of CF₄ (Tables 1 and 2) the latter may be considered the upper limit of influence of C–F stretching on the IR and VCD spectra.

Now let us consider CF₃ in a quite different chiral environment. Fig. 4 shows the IR and VCD spectra of two closely related [2]paracyclo[2](5,8)quinolinophane derivatives of opposite planar AC, namely, (*R_p*)-2,4-dimethyl-[2]paracyclo[2](5,8)quinolinophane [(*R_p*)-11] and (*S_p*)-2-methyl-4-(trifluoromethyl)-[2]paracyclo[2](5,8)quinolinophane [(*S_p*)-7]. Apart from the different planar configuration, in the latter molecule a CF₃ group replaces CH₃ in the 4-position. It was pointed out that AC of a large number of quinolinophane derivatives is unambiguously defined by the (+,+,−) triplet between 1600 and 1500 cm^{−1} associated with (*R_p*), and (−,−,+) triplet associated with (*S_p*) configuration.⁴⁷ This stands out clearly also in Fig. 4.

However, while the VCD and IR spectra of the dimethylquinolinophane (11) do not give any useful information below 1300 cm^{−1} (Fig. 4, left), the presence of the CF₃ group (Fig. 4, right) offers a number of additional pieces of information, counting also two intense IR bands at 1170 and 1120 cm^{−1}, due to mixed normal modes including C–F stretching. A strong VCD couplet is associated to the band at lower IR frequency, whose lower component is negative. The fact that the negative sign is associated with (*S_p*) planar chirality may be at odds with the correspondence (−) \leftrightarrow (*R*) for central chirality. This fact deserves investigating. It is due to the contamination of CF₃-symmetric stretching with other modes of the quinolinophane moiety.



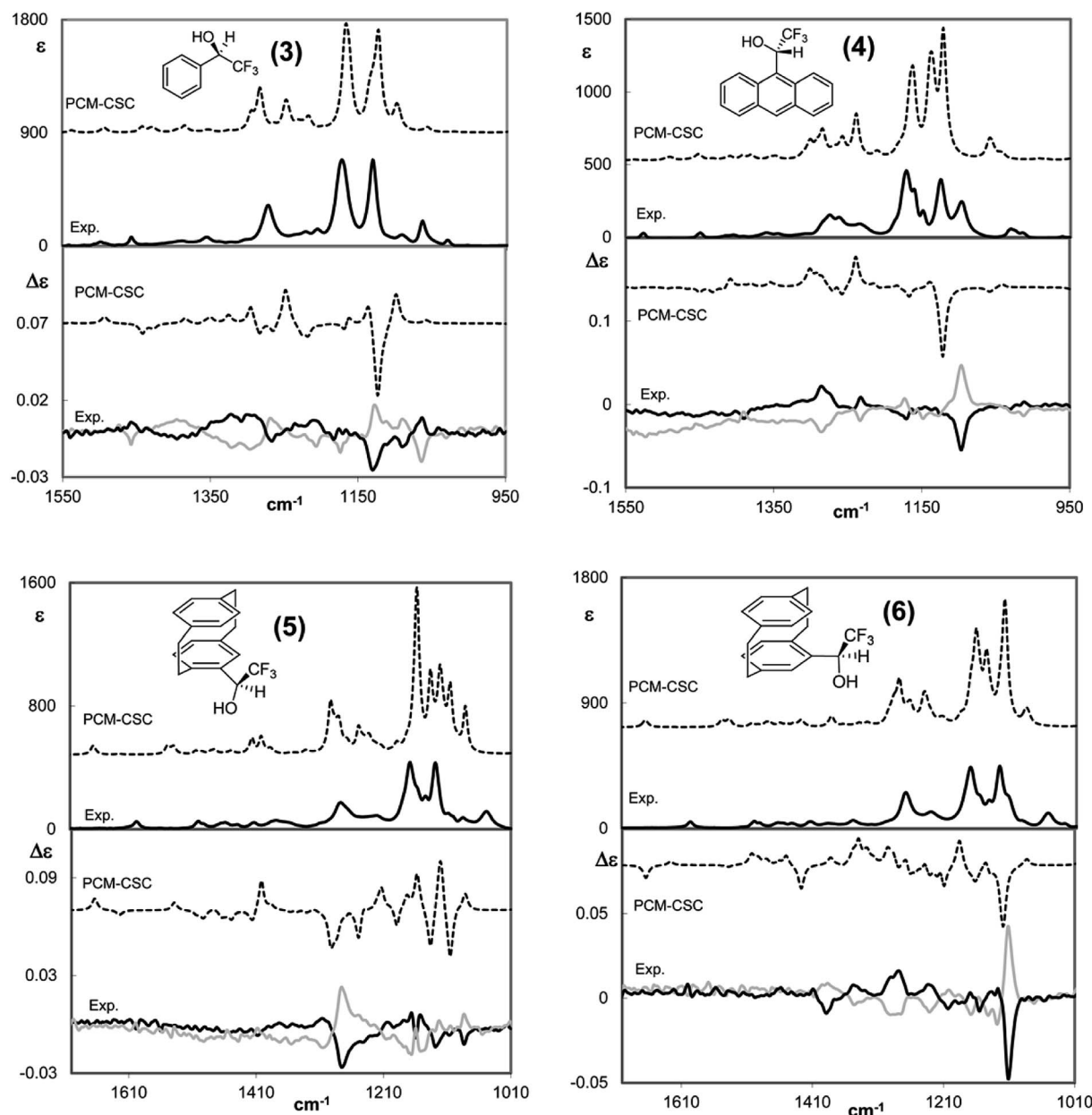


Fig. 3 Comparison of calculated VCD (lower part of each panel) and IR (top part of each panel) spectra of the (*R*)-enantiomers/diastereomers with the corresponding experimental spectra of the (*R*) and (*S*) enantiomers of four chiral aryltrifluorocarbinols, aryl = phenyl, **3** (top left), = anthryl, **4** (top right), and = [2.2]paracyclophan-4-yl, (*R_p*)-**5** and (*S_p*)-**5** (bottom left and right, respectively). Data from ref. 40. No scaling factor applied.

Before moving to the last part of this mini-review, we should remind that remarkable work on CF₃ containing molecules has been carried out by Merten *et al.*, by Monde *et al.* and again by the Polavarapu group.^{48–52}

The last part of this work focuses on two new cases of VCD and IR spectra (compounds **8** and **10** of Scheme 1) with a special attention to C–F stretching modes:

(a) The first case is *N*-*tert*-butanesulfinyl-1-(quinoline-4-yl)-2,2,2-trifluoroethylamine (**8**), which we consider together with the previously studied 1-*tert*-butoxycarbonyl-3-{2-[(*tert*-butanesulfinyl)amino]3,3,3-trifluoropropyl}-1*H*-indole (**9**), both containing a sulfoxide group with well-defined configuration at the

sulfur atom and a stereogenic carbon bearing the CF₃ group. Whilst the chiroptical properties of indole derivative **9** were extensively investigated in our previous work and the AC was correctly assigned,³⁰ for the quinoline **8**, the configuration at sulfur atom only is known. The two diastereomeric (*X,R_S*)- and (*Y,R_S*)-*N*-*tert*-butanesulfinyl-1-(quinoline-4-yl)-2,2,2-trifluoroethylamine compounds (**8**) (see experimental) were separated by simple chromatography on silica gel. In order to assign the AC to the stereogenic carbon of each diastereomer, the same approach based on DFT calculations was adopted, already employed in a previous work.³⁰ However, owing to our increased confidence in handling chiroptical data and



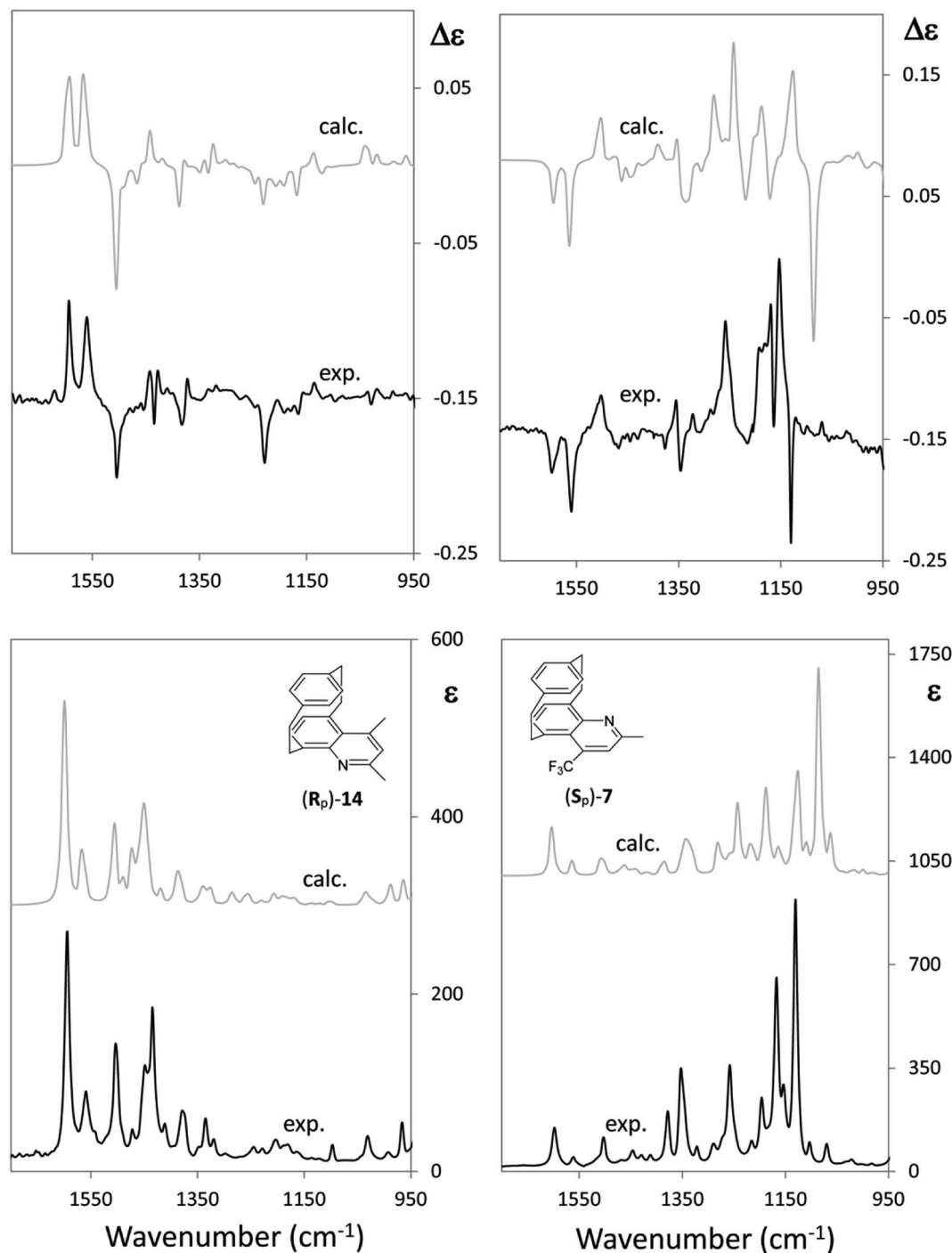


Fig. 4 Comparison of the IR and VCD experimental and calculated spectra of two closely related (*R_p*)-2,4-dimethyl-[2]paracyclo[2](5,8)-quinolinophane [(*R_p*)-**14**] and (*S_p*)-2-methyl-4-(trifluoromethyl)-[2]paracyclo[2](5,8)-quinolinophane [(*S_p*)-**7**] (ref. 47).

stemming from the considerations expounded above, at first, the interpretation of VCD was undertaken by looking at the experimental spectra only. VCD, IR, UV and ECD spectra are reported in Fig. 5; the spectra of each diastereomer having the same configuration at the sulfur atom designated with (*X,R_S*)-**8** and (*Y,R_S*)-**8** are superimposed; IR, VCD UV and ECD spectra for the respective enantiomers (*Y,S_S*)-**8** and (*X,S_S*)-**8** were also taken for a double check.

It should be noted that the UV and IR spectra of (*X,R_S*)-**8** and (*Y,R_S*)-**8** are essentially the same, though they could be different in principle, as for non meso-diastereomers. On the contrary, most of the features of the VCD and ECD spectra are different and show opposite sign, which makes them useful for AC assignment. Based on the previous analysis of VCD feature associated to CF₃-symmetric stretching, a hypothesis of AC assignment can be formulated as follows: in correspondence of the intense IR band at



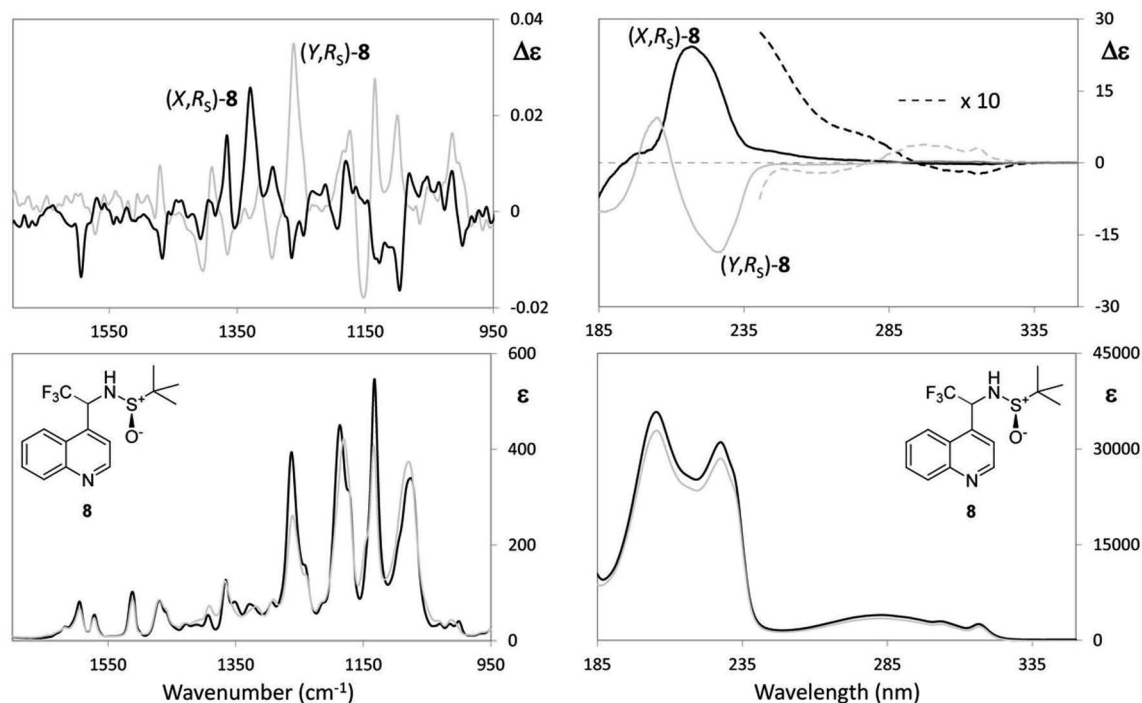


Fig. 5 Left: VCD (top) and IR (bottom) absorption spectra of *N-tert*-butanesulfinyl-1-(quinoline-4-yl)-2,2,2-trifluoroethylamine in CDCl_3 . Right: ECD (top) and UV (bottom) absorption spectra of *N-tert*-butanesulfinyl-1-(quinoline-4-yl)-2,2,2-trifluoroethylamine in CH_3CN . (X,R_S)-**8** (major diastereomer) and (Y,R_S)-**8** (minor diastereomer). Configuration at the sulfur is known, the products being prepared from (R_S)-*tert*-butanesulfinyltrifluoroacetaldehyde (R_S)-**14**. The AC at the stereogenic carbon having to be determined.

$\sim 1130\text{ cm}^{-1}$ (X,R_S)-**8** exhibits a negative broad doublet, indeed, whereas (Y,R_S)-**8** exhibits a positive broad doublet almost enantiomeric to the feature of (X,R_S)-**8**. On the basis of the analysis of the model compounds (3–7) we conclude that the negative feature at 1130 cm^{-1} corresponds to (*R*) configuration and the positive feature at 1130 cm^{-1} corresponds to (*S*) configuration; therefore, the AC of stereomer (X,R_S)-**8** is (R,R_S)-**8**, and that of stereomer (Y,R_S)-**8** is (S,R_S)-**8**. This is confirmed by applying the more rigorous protocol based on DFT calculations¹⁹ and in tune with similar compound **9**.³⁰ In accordance with that approach, we first carry out the conformational analysis of both (R,R_S)- and (S,R_S)-*N-tert*-butanesulfinyl-1-(quinoline-4-yl)-2,2,2-trifluoroethylamine. Results of such analysis are reported in Table 3.

Let us see now if full DFT and TD-DFT calculations provide the same answer. Several conformers are fairly well populated, though their population factors are different depending on whether they are calculated on the basis of either ΔE or ΔG , which means that large amplitude motions have a strong influence.⁵³ In Table 3, the values of three important dihedral angles φ , ψ and θ , are reported: φ denotes the dihedral angle between $\text{F}_3\text{C}-\text{C}$ and $\text{N}-\text{SO}^t\text{Bu}$, ψ refers to the orientation of CF_3 with respect to the aromatic moiety and θ represents the HNC^*CF_3 -dihedral angle. In the most populated conformers, CF_3 is away from both the quinoline moiety and sulfoxide group, whilst it tends to form hydrogen bond with amidic proton NH. The comparison of the calculated VCD spectra of (R,R_S) and of (S,R_S) with the superimposed experimental VCD spectra of (X,R_S)-**8** and (Y,R_S)-**8** is provided in Fig. 6 (the top and bottom part, respectively).

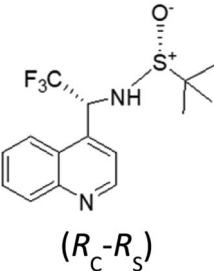
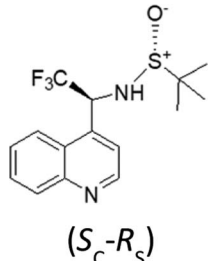
We can see that the band at 1130 cm^{-1} (indicated with diamonds in Fig. 6) is associated with CF_3 stretching and is diagnostic of the configuration of the stereogenic carbon and our above hypothesis about the configurational assignment turns out correct. However, it is worthwhile to notice that also the $(-,+)$ couplet at $\sim 1600\text{ cm}^{-1}$ (indicated with a square in the spectra of Fig. 6), is diagnostic of C^* configuration: DFT calculations show that both the VCD bands at 1130 cm^{-1} and at 1600 cm^{-1} contain a prevalent contribution from the C^*H bending (in Fig. 6 the normal modes for the most populated conformers of (R,R_S)- and (S,R_S)-**8** were considered). However, in the former case C^*H bending combines with CF_3 -low frequency stretchings to a large extent, whereas in the latter case it does not and the corresponding intensity is lower.

The usefulness of VCD and, in particular, of the proposed empirical rule for the sign at $\sim 1150\text{ cm}^{-1}$ VCD band, in discriminating diastereomer configurations is better illustrated in the ESI,[†] where we provide more data for **8** and **9** and also the VCD data for the four diastereomers of a recently synthesized molecule, 2-acetyl-*N*-(*tert*-butanesulfinyl)-3-oxo-1-(trifluoromethyl)butylamine, obtained by Mannich-type addition of 1,3-dicarbonyl compounds to chiral *tert*-butanesulfinyltrifluoroacetaldehydes.⁵⁴

(b) The second new case-study here is 4-[2-(2,2,2-trifluoro-1-hydroxyethyl)pyrrolidin-1-yl]-2-(trifluoromethyl)benzonitrile, **10**: indeed we received from Carbosynth Company an optically inactive product, with unknown diastereomeric composition, possibly a single diastereoisomer with racemic composition, instead of the expected Ligandrol®, the stereomer of (*R,R*) configuration. The chromatographic analysis of that product,



Table 3 Conformational analysis of (*R,R*_S)- and (*S,R*_S)-*N*-*tert*-butanesulfinyl-1-(quinoline-4-yl)-2,2,2-trifluoroethylamine^a

	Conformer	ΔE (% pop)	ΔG (% pop)	φ (°)	ψ (°)	θ (°)
<i>(R,R</i> _S)- <i>N</i> - <i>tert</i> -butanesulfinyl-1-(quinoline-4-yl)-2,2,2-trifluoroethylamine						
	a	0 (60.6)	0 (52.7)	167	82	48
	b	1.10 (9.3)	0.73 (15.3)	131	53	-107
	c	1.82 (2.8)	0.91 (11.3)	96	90	-37
	d	1.01 (9.7)	0.96 (10.5)	138	65	-101
	e	0.92 (12.8)	1.41 (4.8)	171	-102	53
	f	1.92 (2.4)	1.77 (2.6)	78	35	-58
<i>(S,R</i> _S)- <i>N</i> - <i>tert</i> -butanesulfinyl-1-(quinoline-4-yl)-2,2,2-trifluoroethylamine						
	Conformer	ΔE (% pop)	ΔG (% pop)	φ (°)	ψ (°)	θ (°)
	a	1.05 (6.8)	0 (32.5)	-157	-89	73
	b	1.00 (7.4)	0.06 (29.2)	-137	-73	95
	c	0.26 (25.7)	0.50 (14.0)	-108	-89	16
	d	0.60 (14.3)	0.59 (12.0)	-97	-78	140
	e	0 (39.8)	0.89 (7.2)	-93	-24	140
	f	1.43 (3.6)	1.37 (3.2)	-99	102	138

^a Dihedral angles φ , ψ and θ (in degrees) are more precisely defined in the text and denote respectively the orientation of CF₃ with respect to the sulfoxide, to the aryl group and with respect to NH. ΔE and ΔG are expressed in kcal mol⁻¹.

performed on a chiral stationary phase, confirmed our hypothesis. As it is easy to gather from the experimental VCD, IR, ECD and UV spectra of the two eluted compounds shown in Fig. 7, they are enantiomers, given also the opposite specific

rotation values measured immediately after the release of the samples from the column (see Experimental).

As a further proof, the absorption spectra (UV and especially IR) are identical, while the ECD as well as the VCD spectra are

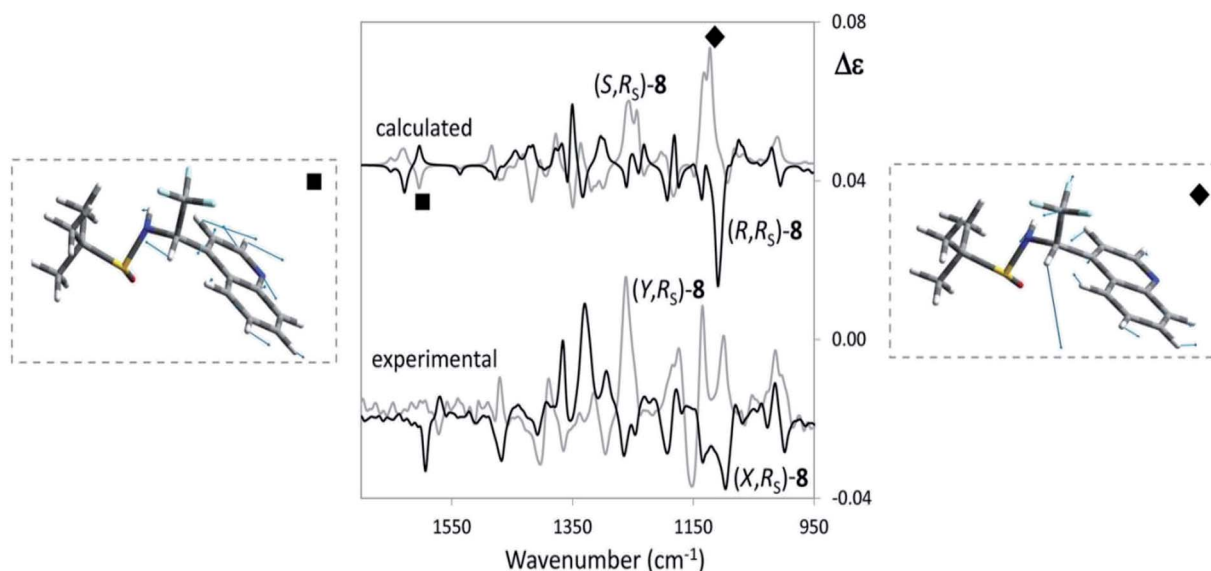


Fig. 6 Comparison of VCD experimental spectra for (*X,R*_S)- and (*Y,R*_S)-*N*-*tert*-butanesulfinyl-1-(quinoline-4-yl)-2,2,2-trifluoroethylamine [(*X,R*_S)- and (*Y,R*_S)-8] with the corresponding calculated spectra of (*R,R*_S)-8 and (*S,R*_S)-8. The comparison allows to conclude that *X* = *R* and *Y* = *S*. Relevant VCD bands for AC assignment are evidenced and the underlying normal mode geometries, as calculated from Gaussian09,²² are depicted.



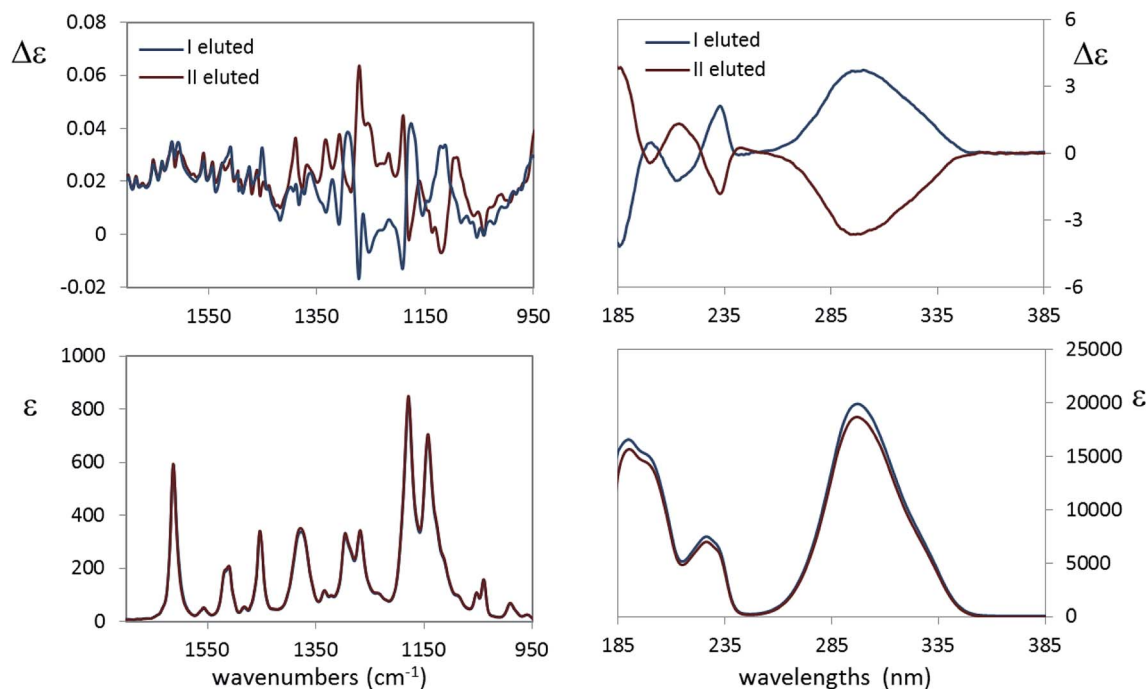


Fig. 7 Left: VCD (top) and IR (bottom) absorption spectra of the two eluted species of 4-[2-2-[1-2,2,2-trifluoro-1-hydroxyethyl]-1-pyrrolidinyl]-2-(trifluoromethyl)benzonitrile, ligand **10** in CDCl_3 . Right: ECD (top) and UV (bottom) absorption spectra of the two eluted species of 4-[2-2-[1-2,2,2-trifluoro-1-hydroxyethyl]-1-pyrrolidinyl]-2-(trifluoromethyl)benzonitrile, ligand **10** in CH_3CN .

definitely mirror images, within the limits of experimental errors. It remains to be discovered whether the original sample is a $(R,R)/(S,S)$ or $(R,S)/(S,R)$ racemic mixture. DFT calculations help solving this dilemma and subsequently checking the above simple empirical rule for the CF_3 -symmetric stretching mode is valid. The free energy and corresponding population factors of the main conformers of the carbinol **10** for the (R,R) and (R,S) configurations respectively are reported in Table 4.

A large number of conformers is predicted for both the (R,R) and (R,S) options, with evident small free energy difference. Many of them arise from the rotation around the N-Ar bond: we observe, indeed, that the conformers in Table 4 come in pairs of almost equal free-energy value, one with the CF_3 group connected to the aromatic ring and in pseudo-*cis* relation with the other CF_3 group and the other pseudo-*trans* to it (cfr. the values of the γ dihedral angle in Table 4 for conformers a and b, c and d etc.). The main difference between the (R,R) and (R,S) option is that the two most populated conformers of the (R,R) stereomer show the OH bond closer to the CF_3 group with a presumable hydrogen bond interaction, whereas, in the two most populated conformers of (R,S) stereomer the OH is directed towards the aromatic ring, as inferred from the angles β and the distance d . The α angle, in most cases close to 180° , allows one to conclude that the $\text{C}_2^*-(\text{CF}_3)$ and the C_1^*-N bonds are antiperiplanar *trans* in most cases. The puckering dihedral angle is negative in most cases, and this implies that the chiral group substituent of the pyrrolidine ring is axial. The comparison of the calculated VCD and IR spectra of the (R,R) and (R,S) configured molecules, scaled in frequency by 0.97, with the corresponding experimental spectra of the first eluted compound is shown in Fig. 8.

Visual inspection of the results in Fig. 8 seems to corroborate the (R,S) configuration assignment to the first eluted diastereomer. However, in order to be more quantitative, and to test the dependence from the scaling factor, we calculated for the

Table 4 Conformational analysis of (R,R) -4-[2-(2,2,2-trifluoro-1-hydroxyethyl)pyrrolidin-1-yl]-2-(trifluoromethyl)benzonitrile [(R,R)-**10**] and (R,S) -4-[2-(2,2,2-trifluoro-1-hydroxyethyl)pyrrolidin-1-yl]-2-(trifluoromethyl)benzonitrile [(R,S)-**10**]^a

CONF	ΔG	% pop	π	α	β	γ	d
(R,R)-a	0.00	26.6	-27.0	-155.6	75.2	-6.2	2.7
(R,R)-b	0.08	23.3	-27.0	-156.7	75.2	170.0	2.7
(R,R)-c	0.47	12.0	-24.8	-159.9	152.1	-8.1	3.2
(R,R)-d	0.60	9.7	18.8	-168.0	81.0	-165.5	2.7
(R,R)-e	0.80	6.9	-24.7	-160.1	150.3	166.8	3.1
(R,R)-f	0.90	5.8	18.8	-167.6	80.4	9.4	2.7
(R,R)-g	1.05	4.5	-27.5	-156.4	-65.9	169.3	2.6
(R,R)-h	1.30	3.0	-27.7	-155.6	-65.5	-5.7	2.6
(R,S)-a	0.00	39.0	-30.6	-151.7	167.7	154.8	3.2
(R,S)-b	0.26	25.3	-30.3	-151.0	168.1	-17.4	3.2
(R,S)-c	1.05	6.7	-35.4	175.7	-71.4	-9.7	2.7
(R,S)-d	1.11	6.0	-35.2	177.0	-72.9	164.8	2.7
(R,S)-e	1.35	4.0	-31.2	-80.4	75.9	-8.8	2.7
(R,S)-f	1.38	3.8	-27.7	68.8	-69.2	173.6	2.6
(R,S)-g	1.49	3.2	-35.0	-146.9	73.9	175.6	2.7
(R,S)-h	1.50	3.1	-31.4	-80.9	76.4	165.9	2.7
(R,S)-i	1.53	3.0	-27.8	68.0	-69.8	-2.1	2.6

^a Dihedral angles: pucker (π : NC_1^*CC), α : $\text{C}(\text{CF}_3)\text{C}_2^*\text{C}_1^*\text{N}$, β : $\text{HOC}_1^*\text{C}(\text{CF}_3)$, γ : $\text{C}_1^*\text{NC}(\phi)\text{C}(\text{CF}_3)$ are in degrees, while the distance $d_{\text{H}(\text{O})-\text{CF}_3}$ (d) is in Å. Free-energies are expressed in kcal mol^{-1} . Significant reported conformers cover ca. 95% of overall populations.



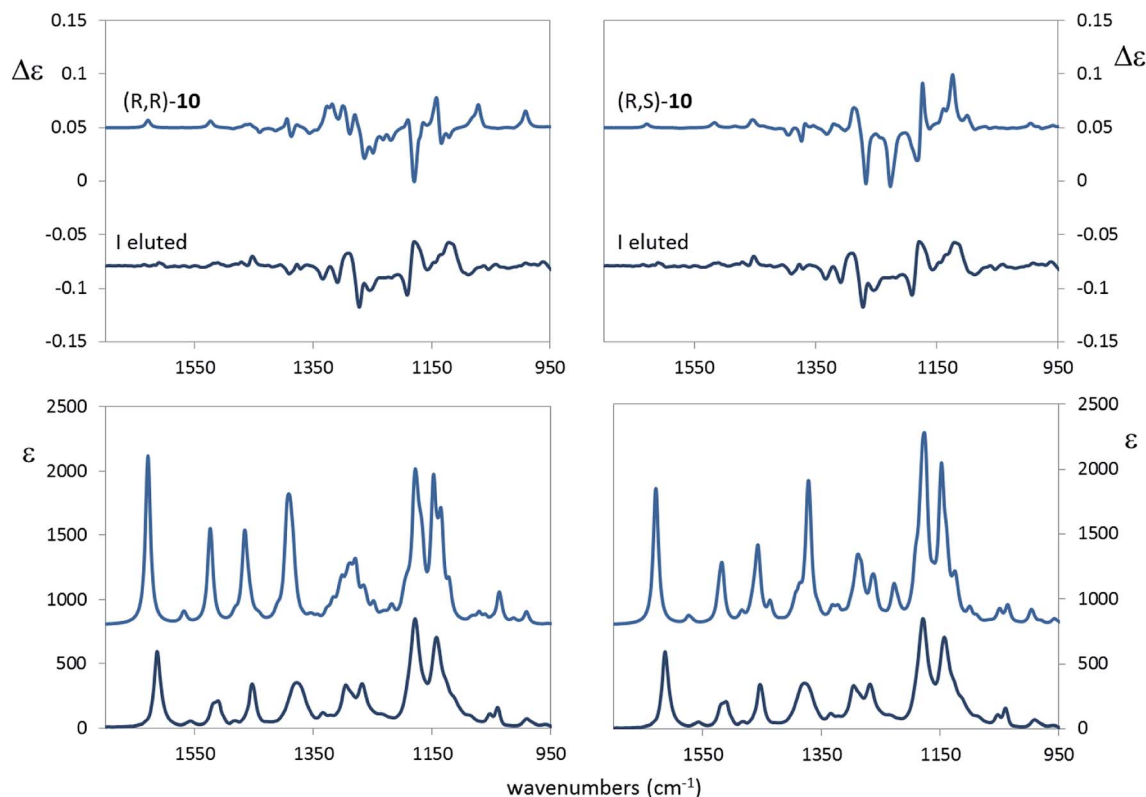


Fig. 8 Left: comparison of calculated VCD (top) and IR (bottom) absorption spectra of *(R,R)*-10 with the corresponding experimental spectra in CDCl_3 for the first eluted compound. Right: comparison of calculated VCD (top) and IR (bottom) absorption spectra of *(R,S)*-10 with the corresponding experimental spectra in CDCl_3 for the first eluted compound. In both cases 0.97 scaling factor was applied to the calculated spectra.

VCD and IR spectra the similarity S.I. index⁵⁵ and the Sim_NN index,⁵⁶ critically discussed also in ref. 17. Results in Table 5 show that the *(R,S)* assignment to the first eluted sample we proposed above is better than *(R,R)*, since larger S.I. and Sim_NN values are calculated for the former choice than for the latter. The 0.97 scaling factor is optimal; from the same table we infer, implicitly, that correlating to the experimental data of the first eluted compound the calculated VCD spectra of either the *(S,S)* or *(S,R)* choice is wrong, since negative indexes would be obtained in those case.

A closer examination of the results in Fig. 8 induces us to pay attention to the characteristic IR doublet at 1160 and 1140 cm^{-1} corresponding respectively to the CF_3 antisymmetric and CF_3 symmetric modes, respectively, somewhat coupled to other vibrational modes. Noteworthy, the VCD band corresponding to the latter component is positive for the first eluted compound. It is reassuring that the correspondence *(R,S)* \leftrightarrow 1st eluted compound obeys the empirical rule we proposed in this work, *i.e.* the VCD band of the CF_3 symmetric mode is positive for the *(S)* configuration of the stereogenic carbon; we also notice that

Table 5 S.I. and Sim_NN indexes for VCD and IR spectra calculated for *(R,R)*-10 and *(R,S)*-10 versus the corresponding experimental spectra of the first eluted compound 10, as function of the scaling factor (value of the latter quantity reported in parenthesis)

VCD						
Isomer	S.I.(1.00)	S.I.(0.99)	S.I.(0.98)	S.I.(0.97)	S.I.(0.96)	S.I.(0.95)
RR	0.24	0.22	0.33	0.04	0.13	0.21
RS	0.40	0.23	0.49	0.69	0.27	0.24
Isomer	Sim_NN(1.00)	Sim_NN(0.99)	Sim_NN(0.98)	Sim_NN(0.97)	Sim_NN(0.96)	Sim_NN(0.95)
RR	0.14	0.12	0.20	0.02	0.07	0.11
RS	0.23	0.12	0.30	0.49	0.15	0.13
IR						
Isomer	S.I.(1.00)	S.I.(0.99)	S.I.(0.98)	S.I.(0.97)	S.I.(0.96)	S.I.(0.95)
RR	0.60	0.63	0.75	0.90	0.86	0.71
RS	0.59	0.64	0.78	0.84	0.81	0.67
Isomer	Sim_NN(1.00)	Sim_NN(0.99)	Sim_NN(0.98)	Sim_NN(0.97)	Sim_NN(0.96)	Sim_NN(0.95)
RR	0.39	0.41	0.52	0.70	0.65	0.48
RS	0.36	0.41	0.55	0.61	0.58	0.43



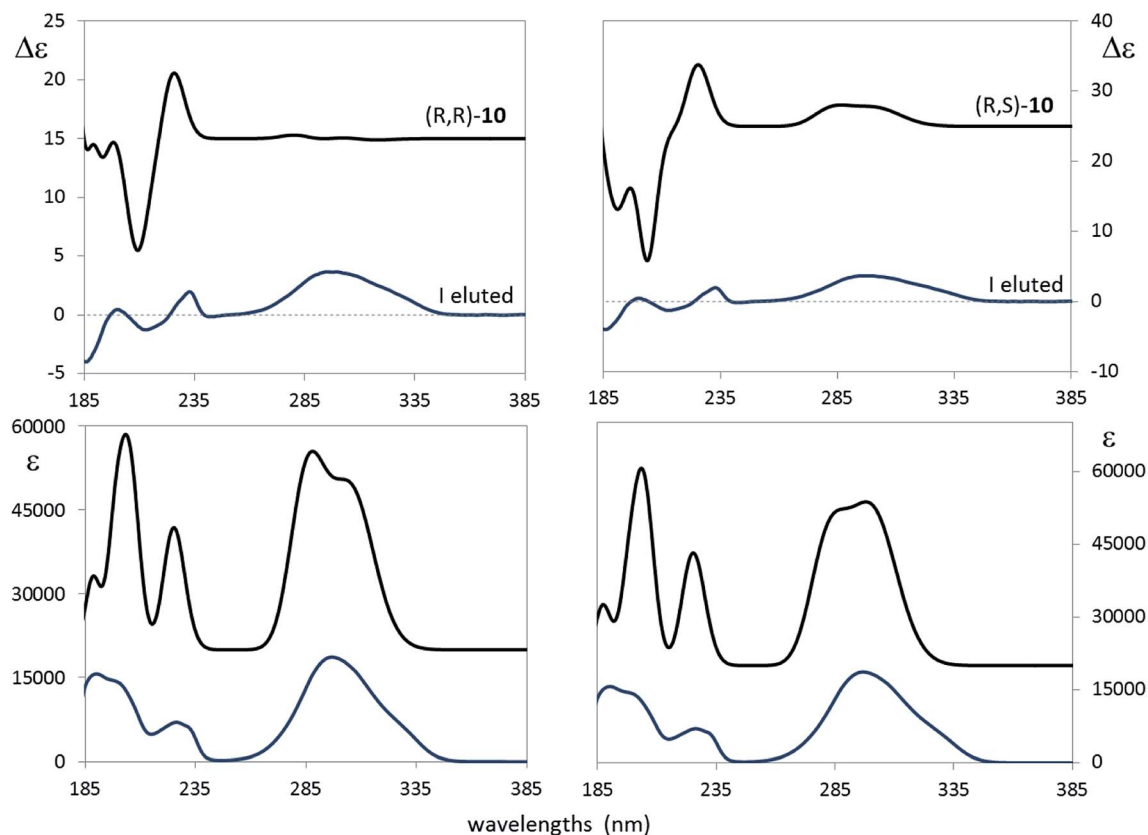


Fig. 9 Left: comparison of calculated ECD (top) and UV (bottom) absorption spectra of *(R,R)*-**10** with the corresponding experimental spectra in CH₃CN for the first eluted compound. Right: comparison of calculated VCD (top) and IR (bottom) absorption spectra of *(R,S)*-**10** with the corresponding experimental spectra in CH₃CN for the first eluted compound. In both cases 20 nm red-shift was applied to the calculated spectra.

this rule does neither imply nor require the OH and CF₃ groups originating a hydrogen bond interaction.

As a final assessment of the just proposed assignment, let us look at Fig. 9, where the calculated ECD and UV spectra of *(R,R)*-**10** and *(R,S)*-**10** are compared with the experimental spectra of the first eluted compound. As described in the Experimental section, calculations in the PCM approximation were run keeping into account acetonitrile as the solvent; consequently a somewhat different conformer distribution of the same conformers of Table 4 was obtained. Fig. 9 suggests once again to favor the *(R,S)* option over the *(R,R)*. Thus we conclude that what we had bought from Carbosynth was the racemic mixture of *(R,S)*-**10** and of *(S,R)*-**10**.

Conclusions

In this work we have reviewed the IR and VCD spectra of a set of *ca.* ten representative chiral compounds containing the CF₃ group, largely present in several important drugs, particularly, aryltrifluoromethylcarbinols CF₃-C*-H ArC*H(CF₃)OH. The literature includes about 20 of these cases and we propose here an empirical rule to assign the absolute configuration, based on the sign of a VCD band, which applies in most cases. Indeed the band for the CF₃-stretching, occurring at *ca.* 1150 cm⁻¹, has a quite intense IR and VCD band, whose sign is diagnostic of the

configuration at the stereogenic carbon C*: (–) for (*R*) and (+) for (*S*) configuration. The same bands have been investigated in other molecular contexts. The above empirical finding, which is somewhat independent on conformations, might prove quite useful to the organic chemists, and is backed by DFT calculations. Exceptions to the rule might occur when the spectroscopic region around 1150 cm⁻¹ is particularly congested with other vibrational transitions, which couple with the low-energy CF₃-stretching, significantly altering its interactions with the surrounding groups and for this reason changing its VCD response. The empirical rule was useful to assess the configurational assignment of two new cases, namely *N*-*tert*-butanesulfinyl-1-(quinoline-4-yl)-2,2,2-trifluoroethylamine and 4-[2-(2,2,2-trifluoro-1-hydroxyethyl)pyrrolidin-1-yl]-2-(trifluoromethyl)benzonitrile. For the latter the use of VCD data and in particular of the proposed empirical rule is efficacious in helping one establish the absolute configuration to be either (*R,S*) or (*S,R*) for a product which is on the market, while the drug ligandrol®, with the same chemical formula, is claimed to be (*R,R*).

Finally we wish to report that, while reviewing the existing VCD literature for CF₃-containing compounds, we realized that quite a few such studies exist. Thus there is ample room for future investigations of this sort, starting possibly from CF₃-substituted steroids, which have paved the way to chiroptical



techniques, as of the seminal studies by Djerassi,⁵⁷ but have not been sufficiently considered by VCD. Another ground to be soon investigated should be the study of fluorine based NMR shift reagents, like Eu(fod)₃.⁵⁸

Conflicts of interest

There are no conflicts to declare.

Acknowledgements

We are grateful to University of Brescia for supporting this work, under the auspices of International Activities program. We wish also to acknowledge the use of computer and software facilities at CINECA-Bologna, Italy, and Regione Lombardia for the LISA grant "LI08p_ChiPhyto", HPL13POZE1.

Notes and references

- (a) Y. Zhou, J. Wang, Z. Gu, S. Wang, W. Zhu, J. L. Aceña, V. A. Soloshonok, K. Izawa and H. Liu, *Chem. Rev.*, 2016, **116**, 422–518; (b) V. Prakash Reddy, *Organofluorine Compounds in Biology and Medicine*, Elsevier, 2015; (c) J. Wang, M. Sánchez-Roselló, J. L. Aceña, C. del Pozo, A. E. Sorochinsky, S. Fustero, V. A. Soloshonok and H. Liu, *Chem. Rev.*, 2014, **114**, 2432–2506; (d) T. Yamazaki, T. Taguchi and I. Ojima, Unique Properties of Fluorine and their Relevance to Medicinal Chemistry and Chemical Biology, in *Fluorine in Medicinal Chemistry and Chemical Biology*, ed. I. Ojima, Wiley, 2009; (e) *Fluorine and Health*, ed. Tressaud and G. Haufe, Elsevier, 2008; (f) *Fluorine in Pharmaceutical and Medicinal Chemistry*, ed. V. Gouverneur and K. Müller, Imperial College Press, 2012.
- M. Gussoni, S. Abbate and G. Zerbi, Prediction of Infrared and Raman Intensities by Parametric Methods, in *Vibrational Spectroscopy. Modern Trends*, ed. A. J. Barnes and W. J. Orville Thomas, Elsevier, Amsterdam, ch. 14, 1977.
- W. B. Person, Infrared Intensities and Atomic Polar Tensors. Ch.4, and: Prediction of infrared Intensities by Transfer of Atomic Polar tensors. Ch. 14, in *Vibrational Intensities in Infrared and Raman Spectroscopies*, ed. W. B. Person and G. Zerbi, Elsevier, Amsterdam, 1982.
- M. Gussoni, Infrared Intensities by Parametric Methods; A Guided Tour. Ch. 5, in *Vibrational Intensities in Infrared and Raman Spectroscopies*, ed. W. B. Person and G. Zerbi, Elsevier, Amsterdam, 1982.
- S. Kondo, Y. Koga, T. Nakanaga and S. Saeki, *Bull. Chem. Soc. Jpn.*, 1983, **56**, 416–421.
- J. H. Newton and W. B. Person, *J. Chem. Phys.*, 1976, **64**, 3036–3049.
- S. Kondo, T. Nakanaga and S. Saeki, *J. Chem. Phys.*, 1980, **73**, 5409–5418.
- K. Kim and W. T. King, *J. Chem. Phys.*, 1980, **73**, 5591–5597.
- J. H. Newton, R. A. Levine and W. B. Person, *J. Chem. Phys.*, 1977, **67**, 3282–3288.
- A. F. Silva, W. E. Richter, A. B. M. S. Bassi and R. E. Bruns, *Phys. Chem. Chem. Phys.*, 2015, **17**, 30378–30388.
- W. E. Richter, L. J. Duarte, A. F. Silva and R. E. Bruns, *J. Braz. Chem. Soc.*, 2016, **27**, 979–991.
- A. Milani, J. Zanetti, C. Castiglioni, E. Di Dedda, S. Radice, G. Canil and C. Tonelli, *Eur. Polym. J.*, 2012, **48**, 391–403.
- S. Abbate and M. Gussoni, *Chem. Phys.*, 1979, **40**, 385–395.
- S. Kondo and S. Saeki, *J. Chem. Phys.*, 1982, **76**, 809–816.
- K. Kim and C. W. Park, *Bull. Korean Chem. Soc.*, 1987, **8**, 174–179.
- L. A. Nafie, *Vibrational Optical Activity: Principles and Applications*, John Wiley and Sons, New York, NY, 2011.
- P. L. Polavarapu, *Chiroptical Spectroscopy. Fundamentals and Applications*, CRC Press, Boca Raton, FL, 2017.
- T. A. Keiderling and A. Lakhani, *Chirality*, 2018, **30**, 238–253.
- P. J. Stephens, F. J. Devlin and J. R. Cheeseman. *VCD Spectroscopy for Organic Chemists*, CRC Press, Boca Raton, FL, 2012.
- P. J. Stephens, *J. Phys. Chem.*, 1985, **89**, 748–752.
- J. Tomasi, B. Mennucci and R. Cammi, *Chem. Rev.*, 2005, **105**, 2999–3094.
- M. J. Frisch, G. W. Trucks, H. B. Schlegel, G. E. Scuseria, M. A. Robb, J. R. Cheeseman, G. Scalmani, V. Barone, B. Mennucci, G. A. Petersson, H. Nakatsuji, M. Caricato, X. Li, H. P. Hratchian, A. F. Izmaylov, J. Bloino, G. Zheng, J. L. Sonnenberg, M. Hada, M. Ehara, K. Toyota, R. Fukuda, J. Hasegawa, M. Ishida, T. Nakajima, Y. Honda, O. Kitao, H. Nakai, T. Vreven, J. A. Montgomery Jr, J. E. Peralta, F. Ogliaro, M. Bearpark, J. J. Heyd, E. Brothers, K. N. Kudin, V. N. Staroverov, R. Kobayashi, J. Normand, K. Raghavachari, A. Rendell, J. C. Burant, S. S. Iyengar, J. Tomasi, M. Cossi, N. Rega, J. M. Millam, M. Klene, J. E. Knox, J. B. Cross, V. Bakken, C. Adamo, J. Jaramillo, R. Gomperts, R. E. Stratmann, O. Yazyev, A. J. Austin, R. Cammi, C. Pomelli, J. W. Ochterski, R. L. Martin, K. Morokuma, V. G. Zakrzewski, G. Voth, P. Salvador, S. Dannenberg, S. Dapprich, A. D. Daniels, Ö. Farkas, J. B. Foresman, J. V. Ortiz, J. Cioslowski and D. J. Fox, *Gaussian 09, Revision A.02*, Gaussian, Inc., Wallingford CT, 2009.
- P. L. Polavarapu, E. A. Donahue, G. Shanmugam, G. Scalmani, E. K. Hawkins, C. Rizzo, I. Ibnuasud, G. Thomas, D. Habel and D. Sebastian, *J. Phys. Chem. A*, 2011, **115**, 5665–5673.
- P. Scafato, F. Caprioli, L. Pisani, D. Padula, F. Santoro, G. Mazzeo, S. Abbate, F. Lebon and G. Longhi, *Tetrahedron*, 2013, **69**, 10752–10762.
- (a) K. Izawa, J. L. Aceña, J. Wang, V. A. Soloshonok and H. Liu, *Eur. J. Org. Chem.*, 2016, **16**; (b) W. K. Hagmann, *J. Med. Chem.*, 2008, **51**(15), 4359–4369; (c) H.-J. Böhm, D. Banner, S. Bendels, M. Kansy, B. Kuhn, K. Müller, U. Obst-Sander and M. Stahl, *ChemBioChem*, 2004, **5**, 637–643.
- For books or reviews, see: (a) *Fluorinated Pharmaceuticals: Advances in Medicinal Chemistry*, ed. A. D. Westwell, Future Science, 2015; (b) E. P. Gillis, K. J. Eastman, M. D. Hill, D. J. Donnelly and N. A. Meanwell, *J. Med. Chem.*, 2015, **58**(21), 8315–8359; (c) *Fluorine in Pharmaceutical and Medicinal Chemistry: From Biophysical Aspects to Clinical*



- Applications*, ed. V. Gouverneur, and Klaus Muller, 1st edn, Imperial College Press, 2012; (d) J.-P. Bégue and D. Bonnet-Delpon, *Bioorganic and Medicinal Chemistry of Fluorine*, 1st edn, Wiley, 2008.
- 27 W. Zhu, J. Wang, S. Wang, Z. Gu, J. L. Aceña, K. Izawa, H. Liu and V. A. Soloshonok, *J. Fluorine Chem.*, 2014, **167**, 37–54.
 - 28 R. Ruzziconi, S. Spizzichino, A. Mazzanti, L. Lunazzi and M. Schlosser, *Org. Biomol. Chem.*, 2010, **8**, 4463–4471.
 - 29 E. C. Sherer, C. H. Lee, J. Shpungin, J. F. Cuff, C. Da, R. Ball, R. Bach, A. Crespo, X. Gong and C. J. Welch, *J. Med. Chem.*, 2014, **57**, 477–494.
 - 30 G. Mazzeo, G. Longhi, S. Abbate, M. Palomba, L. Bagnoli, F. Marini, C. Santi, J. Han, V. A. Soloshonok, E. Di Crescenzo and R. Ruzziconi, *Org. Biomol. Chem.*, 2017, **15**, 3930–3937.
 - 31 T. Bruhn, A. Schaumlöffel, Y. Hemberger and G. Bringmann, *Chirality*, 2013, **25**, 243–249.
 - 32 N. N. Kreienborg and C. Merten, *Phys. Chem. Chem. Phys.*, 2019, **21**, 3506–3511.
 - 33 P. L. Polavarapu, A. L. Cholli and G. Vernice, *J. Am. Chem. Soc.*, 1992, **114**, 10953–10955.
 - 34 J. Kong, L. A. Joyce, J. Liu, T. M. Jarrell, J. C. Culberson and E. C. Sherer, *Chirality*, 2017, **29**, 854–864.
 - 35 T. B. Freedman, X. Cao, L. A. Nafie, A. Solladié-Cavallo, L. Jierri and L. Bouerat, *Chirality*, 2004, **16**, 467–474.
 - 36 O. McConnell, Y. He, L. Nogle and A. Sarkahian, *Chirality*, 2007, **19**, 716–730.
 - 37 P. L. Polavarapu, C. Zhao, A. S. Cholli and G. G. Vernice, *J. Phys. Chem. B*, 1999, **103**, 6127–6132.
 - 38 P. L. Polavarapu, L. P. Fontana and H. E. Smith, *J. Am. Chem. Soc.*, 1986, **108**, 94–99.
 - 39 L. A. Rozov, P. W. Rafalko, S. M. Evans, L. Brockunier and K. Ramig, *J. Org. Chem.*, 1995, **60**, 1319–1325.
 - 40 S. Abbate, F. Lebon, S. Lepri, G. Longhi, R. Gangemi, S. Spizzichino, G. Bellachioma and R. Ruzziconi, *ChemPhysChem*, 2011, **12**, 3519–3523.
 - 41 L. A. Nafie, T. A. Keiderling and P. J. Stephens, *Vibrational Circular Dichroism*, *J. Am. Chem. Soc.*, 1976, **98**, 2715–2723.
 - 42 V. M. Pultz, *Vibrational Circular Dichroism Studies of Some Small Chiral Molecules*, PhD Thesis, University of Minnesota, 1983.
 - 43 M. G. Paterlini, T. B. Freedman and L. A. Nafie, *J. Am. Chem. Soc.*, 1986, **108**, 1389–1397.
 - 44 D. M. P. Gigante, F. Long, L. A. Bodack, J. M. Evans, J. Kallmerten, L. A. Nafie and T. B. Freedman, *J. Phys. Chem. A*, 1999, **103**, 1523–1537.
 - 45 M. Passarello, S. Abbate, G. Longhi, S. Lepri, R. Ruzziconi and V. P. Nicu, *J. Phys. Chem. A*, 2014, **118**, 4339–4350.
 - 46 F. Hof, D. M. Scofield, W. B. Schweizer and F. Diederich, *Angew. Chem., Int. Ed.*, 2004, **116**, 5166–5169.
 - 47 G. Mazzeo, G. Longhi, S. Abbate, F. Buonerba and R. Ruzziconi, *Eur. J. Org. Chem.*, 2014, 7353–7363.
 - 48 C. Merten, K. J. Jalkanen, V. C. Weiss and A. Hartwig, *Chirality*, 2010, **22**, 772–777.
 - 49 K. Monde, N. Miura, M. Hashimoto, T. Taniguchi and T. Inabe, *J. Am. Chem. Soc.*, 2006, **128**, 6000–6001.
 - 50 F. Wang, P. L. Polavarapu, V. Schurig and R. Schmidt, *Chirality*, 2002, **14**, 618–624.
 - 51 P. L. Polavarapu, C. Zhao and K. Ramig, *Tetrahedron: Asymmetry*, 1999, **10**, 1099–1106.
 - 52 C. D. Tran, V. I. Grishko and G. Huang, *Anal. Chem.*, 1994, **66**, 2630–2635.
 - 53 G. Longhi, S. Abbate, P. Scafato and C. Rosini, *Phys. Chem. Chem. Phys.*, 2010, **12**, 4725–4732.
 - 54 G. Mazzeo, G. Longhi, S. Abbate, F. Mangiavacchi, C. Santi, J. Han, V. A. Soloshonok, L. Melensi and R. Ruzziconi, *Org. Biomol. Chem.*, 2018, **16**, 8742–8750.
 - 55 T. Kuppers, W. Langenaeker, J. P. Tollenaere and P. Bultinck, *J. Phys. Chem. A*, 2003, **107**, 542–553.
 - 56 J. Shen, C. Zhu, S. Reiling and R. Vaz, *Spectrochim. Acta, Part A*, 2010, **76**, 418–422.
 - 57 C. Djerassi, *Steroids*, in *Optical Rotatory Dispersion*, ed. C. Djerassi, McGraw-Hill, New York, 1960, ch. 4.
 - 58 D. H. Williams, *Pure Appl. Chem.*, 1974, **40**, 25–40.

